



**Federal Aviation
Administration**

DOT/FAA/AM-17/9
Office of Aerospace Medicine
Washington, DC 20591

Assessment of Head and Neck Injury Potential During Aircraft Longitudinal Impacts

Richard L. DeWeese¹
David M. Moorcroft¹
M.M.G.M. Philippens²

¹Civil Aerospace Medical Institute
Federal Aviation Administration
Oklahoma City, OK 73125

²TNO Defense, Security and Safety
2600 JA Delft
The Netherlands

February 2017

Final Report

NOTICE

This document is disseminated under the sponsorship of the U.S. Department of Transportation in the interest of information exchange. The United States Government assumes no liability for the contents thereof.

This publication and all Office of Aerospace Medicine technical reports are available in full-text from the Civil Aerospace Medical Institute's publications website:
<http://www.faa.gov/go/oamtechreports>

Technical Report Documentation Page

1. Report No. DOT/FAA/AM-17/9		2. Government Accession No.		3. Recipient's Catalog No.	
4. Title and Subtitle Assessment of Head and Neck Injury Potential During Aircraft Longitudinal Impacts				5. Report Date February 2017	
				6. Performing Organization Code	
7. Author(s) DeWeese R, ¹ Moorcroft D, ¹ Philippens MMGM ²				8. Performing Organization Report No.	
9. Performing Organization Name and Address ¹ FAA Civil Aerospace Medical Institute P.O. Box 25082, Oklahoma City, OK 73125 ² TNO Defense, Security, & Safety, The Netherlands				10. Work Unit No. (TRAIS)	
				11. Contract or Grant No.	
12. Sponsoring Agency name and Address Office of Aerospace Medicine Federal Aviation Administration 800 Independence Ave., S.W. Washington, DC 20591				13. Type of Report and Period Covered	
				14. Sponsoring Agency Code	
15. Supplemental Notes					
16. Abstract The risk of head-neck injuries was evaluated for certain aircraft seat and interior configurations in aircraft longitudinal impacts. Two loading scenarios for the head-neck system were investigated: inertial (non-contact) loading in posterior-anterior and lateral direction using a forward facing seat and side facing couch, respectively, and contact loading through impacts of the head with typical aircraft interior components. The sled tests simulate an impact along the longitudinal axis of the aircraft; however, the seat orientation causes either forward or lateral occupant loading. The FAA Hybrid III was used in the occupant-forward impacts, and the ES-2 Anthropomorphic Test Device (ATD) was used in the occupant-lateral impacts. The ATDs utilized a unique 9-accelerometer array (NAP) bracket. Techniques were applied to derive rotational acceleration and velocity from the NAP. Head rotational velocities were cross-validated using photometric techniques. Both ATDs were also equipped with upper and lower neck 6-axis load cells. The restraint configurations investigated for inertial loading were a forward facing pilot seat with a 4-point restraint, a forward facing passenger seat with a lap belt restraint, and a side facing passenger seat with a 3-point restraint. The contact load configurations utilized a forward facing passenger seat with a lap belt restraint with either a passenger seat back or simulated class divider as impact surfaces. The neck injury potential was evaluated by the Federal Motor Vehicle Safety Standards Nij criterion, using the neck loads at the occipital condyle level. The NAP data were used to evaluate head injury potential with multiple versions of the Head Injury Criteria (HIC), Skull Fracture Correlate, and the Brain Injury Criteria (BrIC). Neck injury was not a significant risk in most of the forward facing configurations tested; the only test with a Nij value above the limit also exceeded the HIC limit. For the side facing test configurations, neck injury was a significant risk, particularly for seating systems that did not provide effective upper body support. For head injury risk, significant differences were seen between the aviation and automotive versions of HIC. In several tests, aviation HIC was not calculated because there was no contact, but the automotive versions of HIC and BrIC suggest a risk of head injury. Overall, these results indicate that using both HIC and BrIC to evaluate seating systems could provide a safety benefit by directly evaluating the risk of skull fracture and traumatic brain injury.					
17. Key Words HIC, BrIC, Nij, Head Injury, Neck Injury, Aircraft Crash			18. Distribution Statement Document is available to the public through the Internet: http://www.faa.gov/go/oamtechreports/		
19. Security Classif. (of this report) Unclassified		20. Security Classif. (of this page) Unclassified		21. No. of Pages 37	22. Price

ACKNOWLEDGMENTS

The work would not have been completed without the full support of the technical staff at CAMI: David DeSelms, Ronnie Minnick, and Bryan Provine. Erik Takhounts at NHTSA supplied the SIMon software and assisted the authors in implementing it. Robert Trimble of Weber Aircraft supplied the test seats, and Joe McEntire of the U.S. Army Aeromedical Research Laboratory supplied the 4-point restraint systems.

Contents

BACKGROUND.....	1
METHODS.....	2
Forward-Facing Seat Configuration.....	3
Inertial Loading Test Configuration.....	4
Row-to-Row Test Configuration.....	5
Wall Test Configuration.....	7
Side-Facing Seat Configuration.....	9
Test Device.....	10
FAA Hybrid III.....	10
Euro SID 2.....	10
Instrumentation.....	10
Electronic Instrumentation.....	10
Video Coverage.....	11
Injury Evaluations.....	11
Head Injury Criteria (HIC).....	12
Skull Fracture Correlate (SFC).....	12
Brain Injury Criteria (BrIC).....	12
Neck Injury.....	13
RESULTS.....	14
Forward-Facing Seat Configuration.....	14
Inertial Loading Test Configuration.....	14
Row-to-Row Test Configuration.....	15
Side-Facing Seat Configuration.....	19
Center Test Configuration.....	19
Wall Test Configuration.....	20
Armrest Test Configuration.....	21
DISCUSSION.....	23
Neck Injury.....	23
Head Injury.....	23
Brain Injury.....	23
LIMITATIONS.....	25
CONCLUSION.....	26
REFERENCES.....	27
APPENDIX.....	A-1
Angular Velocity Derivation.....	A-1
NAP Calculations.....	A-1
NAP Corrections.....	A-3

ASSESSMENT OF HEAD AND NECK INJURY POTENTIAL DURING AIRCRAFT LONGITUDINAL IMPACTS

BACKGROUND

Current aircraft seat dynamic qualification tests utilize the Head Injury Criteria (HIC) to evaluate head protection. HIC was selected for use because it was the most widely accepted means of head injury assessment when the dynamic seat requirements were adopted in 1988 [1, 2]. The original version of HIC cited in the automotive safety standards, referred to as HIC Unlimited, considered the entire acceleration time history of the impact event and had a pass/fail limit of 1000. A subsequent revision to the National Highway Traffic Safety Administration (NHTSA) rule capped the calculation at 36 ms [3]. The aviation version of the calculation disregards any head acceleration prior to contact with a surface. This adjustment was the Federal Aviation Administration's (FAA) means of compensating for the tendency for HIC to overestimate the injury risk for long periods of relatively low acceleration (as can occur during occupant flail prior to head contact). Since HIC had been originally validated for short duration impacts (less than or equal to 13 ms) that resulted in skull fracture, excluding non-contact acceleration seemed to be a reasonable approach at the time. A version that compensated for this tendency by limiting the length of time considered by the calculation to 15 milliseconds was later adopted in the auto safety standards [4]. This version of HIC, referred to as HIC15, had a lower pass/fail limit of 700. While the defined level of safety provided by HIC has evolved since its introduction, current probability methods define a HIC36 value of 1000 as a 23% chance of a serious injury [5]. That level of head injury can result in unconsciousness from 1-6 hours, which means that occupants may not be alert and able to assist with their own evacuation after a crash. This concern about the ability to self-evacuate, and the emergence of technologies and criteria to assess brain injury risk, was part of the motivation behind completing a project to determine the baseline head injury risk for typical aircraft seats.

Current aircraft seat qualification tests do not assess neck injury potential for several reasons. The original criteria were selected to protect occupants during expected impact scenarios (primarily longitudinal and vertical impact vectors relative to the aircraft) when seated in the most common types of seats (forward and aft facing). The criteria focused on controlling the most serious injuries that were likely to result from those combinations of seat types and impact scenarios. Neck injury was not identified as high risk in those impact scenarios. Neck injury assessment was also not included for one very practical reason, the technology to measure neck loading and an accepted injury criteria to determine neck injury risk did not exist at the time of the rule's adoption. Since that time, technology and injury criteria have been developed to assess neck injuries. The significant neck flexion observed in some impact scenarios is one of the motivating factors for conducting this neck injury risk assessment. Another factor was concern that HIC reduction methods such as energy absorbing seat backs and airbags could have the unintended consequences of inducing injuries to the neck.

METHODS

Head and neck injury potential during forward impacts for occupants of typical aircraft seats and interior configurations was assessed in 26 tests across 6 configurations (Table 1). Two primary loading scenarios were investigated: inertial (non-contact) loading in the posterior-anterior and lateral direction using, respectively, a forward-facing seat and a side-facing couch, and contact loading through impacts of the head with typical aircraft interior components (seatbacks and walls). The aircraft longitudinal impacts were simulated by sled tests conducted at the FAA Civil Aerospace Medical Institute (CAMI) using an FAA Hybrid III and an ES-2 Anthropomorphic Test Device (ATD). The ATDs utilized a unique 9-accelerometer array (NAP) bracket developed by the Netherlands Organisation for Applied Scientific Research (TNO, the Netherlands). The restraint configurations investigated for inertial loading were a forward-facing pilot seat with a 4-point restraint, a forward-facing passenger seat with a 2-point belt restraint, and a side-facing passenger seat with a 3-point restraint. The contact load configurations utilized passenger seat backs, simulated class dividers, and rigid walls as impact surfaces.

Table 1: Test Matrix

Test Number	Seat Orientation	Configuration	Nominal G Peak	ATD	Restraint
A05044	Forward	No Contact	26 G	FAA Hybrid III	4-pt
A05045	Forward	No Contact	26 G	FAA Hybrid III	4-pt
A05046	Forward	No Contact	26 G	FAA Hybrid III	4-pt
A05047	Forward	Torso Contact	16 G	FAA Hybrid III	Lap
A05048	Forward	Torso Contact	16 G	FAA Hybrid III	Lap
A05049	Forward	Seat Back	16 G	FAA Hybrid III	Lap
A05050	Forward	Seat Back	16 G	FAA Hybrid III	Lap
A05051	Forward	Seat Back	16 G	FAA Hybrid III	Lap
A05052	Forward	Seat Back	16 G	FAA Hybrid III	Lap
A05054	Forward	Wall	16 G	FAA Hybrid III	Lap
A05055	Forward	Wall	16 G	FAA Hybrid III	Lap
A05056	Forward	Wall	16 G	FAA Hybrid III	Lap
A05057	Forward	Wall + Ledge	16 G	FAA Hybrid III	Lap
A05058	Forward	Wall + Ledge	16 G	FAA Hybrid III	Lap
A05066	Side	Center	16 G	ES-2	3-pt
A05068	Side	Center	16 G	ES-2	3-pt
A05067	Side	Center	16 G	ES-2	Inflatable
A05070	Side	Center	16 G	ES-2	Inflatable
A05065	Side	Close Wall	16 G	ES-2	3-pt
A05071	Side	Far Wall	16 G	ES-2	3-pt
A05072	Side	Far Wall	16 G	ES-2	3-pt
A05075	Side	Armrest	16 G	ES-2	3-pt
A05076	Side	Armrest	16 G	ES-2	3-pt
A05073	Side	Armrest	16 G	ES-2	Inflatable
A05074	Side	Armrest	16 G	ES-2	Inflatable
A06004	Side	Armrest	16 G	FAA Hybrid III	3-pt

Forward-Facing Seat Configuration

Fourteen tests were completed with a forward-facing seat and an FAA Hybrid III ATD. Typical seating configurations found in both transport and general aviation were chosen based on likelihood of head and/or neck injury. Three configurations were tested: inertial loading that resulted in no contact or dummy-to-dummy contact, row-to-row which resulted in contact with a seatback, and a simulated front row seat with a wall impact. The inertial loading configurations with only a lap belt resulted in torso contact with the upper leg and head contact with the lower leg.

Thirteen tests used a rigid launch seat and no yaw to reduce variability and simplify analysis of results (Figure 1). The seat back angle was 13 degrees to vertical and had no back cushion. The seat pan was 5 degrees from horizontal, with a bottom cushion made from 1 inch of very firm closed cell foam (IV3) covered with cloth. Forward sliding of the cushion was minimized by a positive stop at the front edge of the seat pan. This cushion thickness and stiffness was chosen to maximize test repeatability and is not necessarily representative of an actual aircraft seat cushion. To ensure a consistent initial position, a headrest was positioned to support the head at the nominal (un-flexed) position. The headrest was constructed of a 4.25-inch thick block of polyethylene foam. The ATD was tied back against the headrest with two strands of 4 pound breaking strength string to prevent motion during the sled acceleration phase (Figure 2). The arms were placed a few inches further back than what is used for a typical certification test in an attempt to limit the obscuration of the head photometric targets. The fourteenth test was part of an annual training class taught at CAMI and included a real launch seat, 10 degrees of yaw, and floor misalignment under the impacted seat.

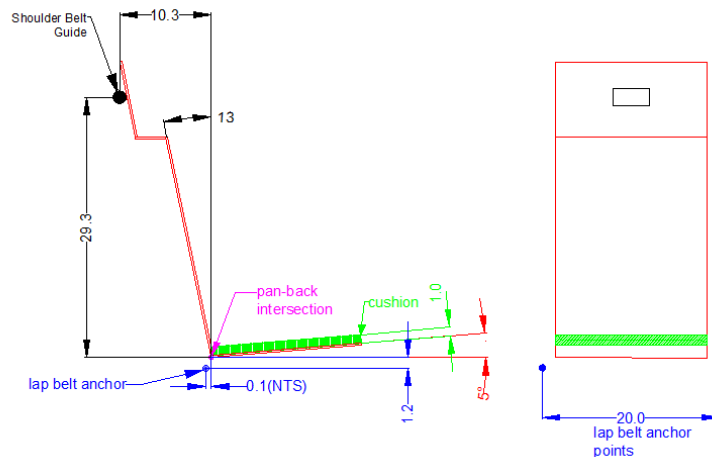


Figure 1: Schematic of Rigid Seat (dimensions in inches)



Figure 2: Breakaway String Installation

Inertial Loading Test Configuration

- Tests A05044 – A05046: 4-point restrained occupant subjected to 14 CFR 23.562 pilot seat 26 G, 42 ft/s forward deceleration [2]. The rigid seat was configured to emulate the seating position and belt anchor location of a typical Part 23 pilot seat (Figure 3). The ATD's feet were placed on simulated rudder pedals and a 4-point UH-1 (military helicopter) harness with no inertia reel was used. The lap belt portion was 3 inches wide, and the shoulder straps were 1.75 inches wide and merged into a single strap behind the neck. The lap belt anchors were 20 inches apart and were 0.1 inch aft and 1.2 inches below the intersection of the seat pan and seat back planes. The shoulder belt guide was 10.3 inches aft and 29.3 inches above the pan/back intersection. All slack was removed from the lap belt, and the shoulder belts were adjusted to provide 1 inch of slack (to emulate typical I-reel payout).

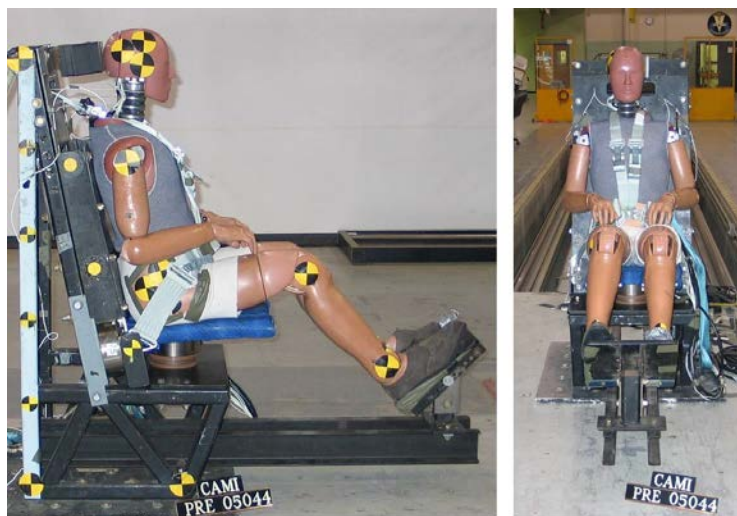


Figure 3: 4-point Belt Test Setup

- Tests A05047 and A05048: Lap belt restrained occupant subjected to a 14 CFR 25.562 16 G, 44 ft/s forward deceleration [1]. The rigid seat was configured to emulate the seating position and belt anchor location of an economy class passenger seat (Figure 4). The floor was 15.6 inches below the pan/back intersection. The belt anchors were 16 inches apart and located 1.15 inches forward and 0.6 inch above the pan/back intersection. A new nylon aircraft passenger lap belt was used for each test. For test A05047, the ATD feet were placed flat on the floor with the toes against a vertical stop 30 inches forward of the pan-back intersection. This test was to determine the unrestricted head path, for use in the subsequent row-to-row tests. For test A05048, the same seat configuration and ATD position was used, but the foot stop was not. A triple place passenger seat was placed well forward of rigid seat, to determine the kinematics of the seat back for use in the subsequent row-to-row tests.



Figure 4: Lap Belt Test Setup

Row-to-Row Test Configuration

- Tests A05049 – A05051: Lap belt restrained occupant subjected to a 14 CFR 25.562 16 G, 44 ft/s forward deceleration impacting an economy-class seat back (Figure 5). The same rigid seat configuration and ATD position as in A05048 was used. A new nylon aircraft passenger lap belt was used for each test. The target seat was a triple place passenger seat frame with a fully dressed seat back in the center position. The seat frame was reinforced to withstand multiple impacts without deformation, and it was inspected for damage after each test. The back had provisions for installation of a video screen just above the tray table. In lieu of the actual screen, a wooden surrogate screen of the same size and shape was installed. This seat back is designed to absorb head impact energy by sequentially shearing a pair of bolts in the hinge mechanism. The energy absorbing (EA) bolts were tightened per the manufacturer’s specifications. The goal of these tests was to have the head strike the center of the seat back, just above the tray table. ATD head path and seatback flexion data determined from photometric analysis of previous tests were used to select the struck seat back fore/aft position that would give the highest probability

of achieving the impact goal. This resulted in the target seat back hinge point located 32.7 inches forward of the rigid seat pan/back intersection. The top of the tray table was 25.8 inches forward and 20.4 inches above the pan/back intersection.

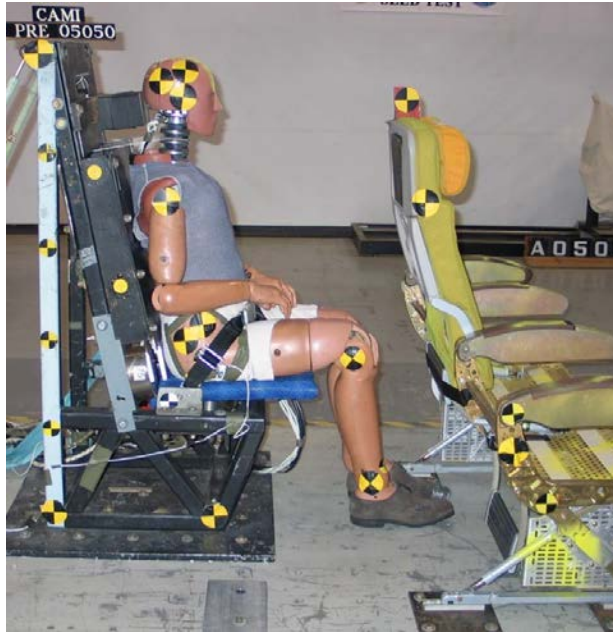


Figure 5: Row-to-Row Test Setup

- Test 05052: Lap belt restrained occupant subjected to a 14 CFR 25.562 16 G, 44 ft/s forward deceleration impacting an economy-class seat energy absorbing seat (Figure 6). The ATD was seated in center place of a passenger triple seat yawed 10 degrees counter clockwise from the aircraft centerline. A new nylon aircraft passenger lap belt was used for each test. The struck seat was a fully occupied passenger triple seat that incorporated stroking rear seat legs intended to limit loads on the seat track during a forward impact. The seat backs incorporated energy absorbing hinge mechanisms similar to the seat backs struck in the previous tests. The seats were installed at a pitch of 30 inches. The ATDs were seated according to standard certification testing methods, including the placement of the arms [6].



Figure 6: Row-to-Row Test with Yaw

Wall Test Configuration

- Lap belt restrained occupant subjected to a 14 CFR 25.562 16 G, 44 ft/s forward deceleration impacting a wall (Figure 7). These five tests used the same seat and ATD position as in the previous rigid seat row-to-row tests. A new nylon aircraft passenger lap belt was used for each test.
- The wall consisted of a 1-inch thick, 24-inch wide by 48-inch tall, fiberglass faced Nomex® honeycomb core panel of the type used in typical aircraft interior walls. Wall panel was clamped across the bottom 3 inches of the panel, and simply supported by rollers across the top. The unsupported height of the panel was 39.25 inches from the top the bottom clamp edge to the middle of the forward roller support. The bottom of the panel was 10.75 inches above the floor. The wall was placed 35 inches forward of the pan/back intersection, which is a common installation distance. A separate floor stop panel was provided at the same plane as the wall. This panel material and mounting configuration was intended to emulate the stiffness of a seating class divider panel.



Figure 7: (L) Wall Test Setup, (R) Close-up of Roller Support

- Tests A05054 – A05056: These three tests used the same wall configuration except for the location of the aft roller (Figure 7). In tests A05055 and A05056, the roller was raised 1 inch with respect to the forward roller to increase the stiffness of the upper end condition.
- Tests A05057 and A05058: These two tests with the same wall configuration as A05056. A rigid surface was placed in the path of the head such that after the head interaction with the wall was over, the head would strike the surface (Figure 8). The goal of this test was to evaluate the effect of two successive head impacts. For test A05057, the secondary strike surface was a 4-inch wide, 0.25-inch thick steel angle padded with 2 inches of IV3 foam, parallel to the wall with the top 16.75 inches from the floor. The aft roller was raised 4 inches with respect to the front roller to further increase the stiffness of the upper end condition. For test A05058, the secondary strike surface was an 8-inch wide, 4-inch deep horizontal surface padded with 2 inches of IV3 foam. Top surface was 18.5 inches from the floor. The aft roller was placed at the same level as the front roller, minimizing the stiffness of the upper panel end condition.

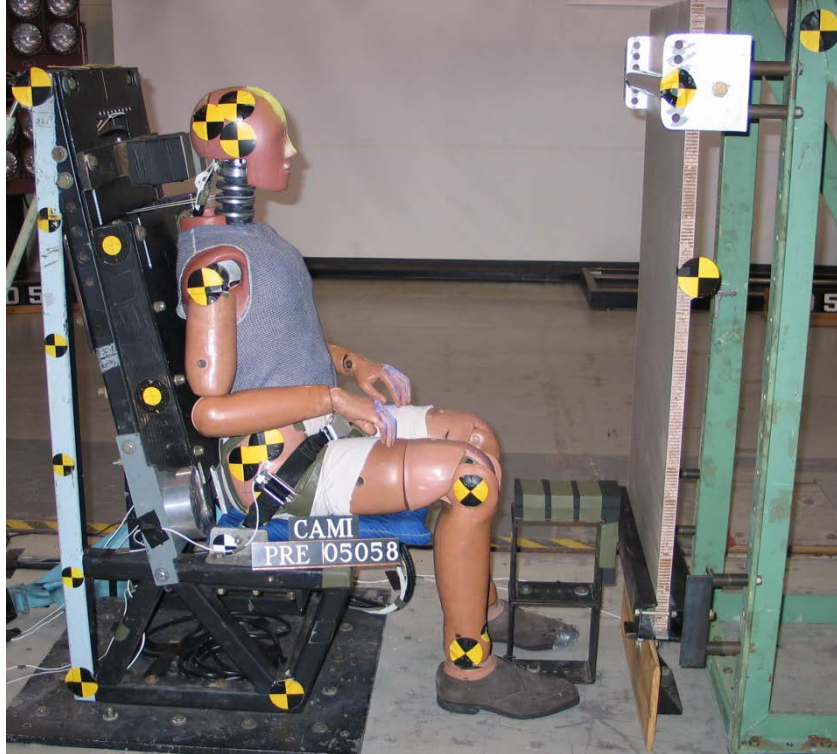


Figure 8: Wall Test with Secondary Strike Surface

Side-Facing Seat Configuration

Eleven tests were completed with a side-facing seat as part of a project to evaluate the ES-2 side-impact dummy [7]. Three configurations were tested: center position (non-contact), seated next to a rigid wall, and seated next to an armrest (Figure 9). All tests were subjected to the 14 CFR 25.562 16 G, 44 ft/s forward deceleration. Each configuration included a body centered 3-point seat belt, six tests with a conventional belt and five tests with an inflatable torso restraint. Some tests were repeated to assess data spread. Ten tests used the ES-2 ATD and the eleventh test used the FAA Hybrid III.

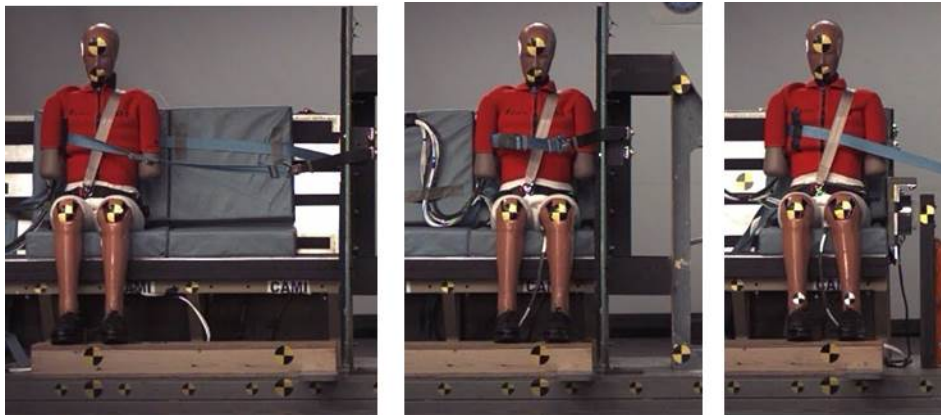


Figure 9: ES-2 Test Setups with Conventional Restraints

Test Device

FAA Hybrid III

The FAA Hybrid III differs from the standard Hybrid III used in automotive testing because it has been modified to better emulate the more upright posture of an occupant in an airliner seat and provide kinematic and vertical response equivalent to the Hybrid II [8]. The modification consists of several Hybrid II parts substituted into the structure including the lumbar spine, abdominal insert, chest jacket, and upper leg bone. FAA regulations require certification tests be performed with the Hybrid II or an equivalent and the FAA Hybrid III has been deemed equivalent [9]. The FAA Hybrid III was selected because it is capable of measuring neck loads while the Hybrid II cannot.

Euro SID 2

The ES-2 ATD is specially designed to evaluate injury in test conditions with significant lateral loading. This ATD is cited in FAA policy PS-ANM-25-03-R1 for side facing seats and 49 CFR 571.214 for use in automotive side impact tests [10, 11]. The dummy exhibits good biofidelity when used to evaluate typical aviation seat configurations [7]. While the policy and regulation above cite the 49 CFR Part 572 subpart U [12], referred to as the ES-2re, the research cited herein was conducted with an ES-2 build level E2.AI. The ES-2re has a set of rib extensions that extend from the ends of the ribs to the back plate, filling a gap that had existed in the previous version. These extensions improved the consistency of the interaction with contoured seat back upholstery common in automobiles [13]. Since the back upholstery used in the FAA research test seats was not contoured, it is unlikely that using the ES-2re in these tests would have produced a different response than the original ES-2.

Instrumentation

Electronic Instrumentation

Both the FAA Hybrid III and ES-2 were instrumented with a nine-accelerometer array package (NAP) to allow for the calculation of angular head acceleration and velocity. The array mount and computational algorithm were provided by TNO. The mount, shown in Figure 10, was designed to reduce resonant responses and dynamic location inaccuracies found in some other NAP arrangements. The angular acceleration and velocity were derived using measured differential linear accelerations and the NAP geometry via a computational algorithm implemented in Matlab [See Appendix]. This mount weighed 0.46 pound (without accelerometers) versus the 0.28 pound weight of the standard accelerometer block that it replaced. The ATDs were also instrumented with upper and lower 6-axis neck load cells.

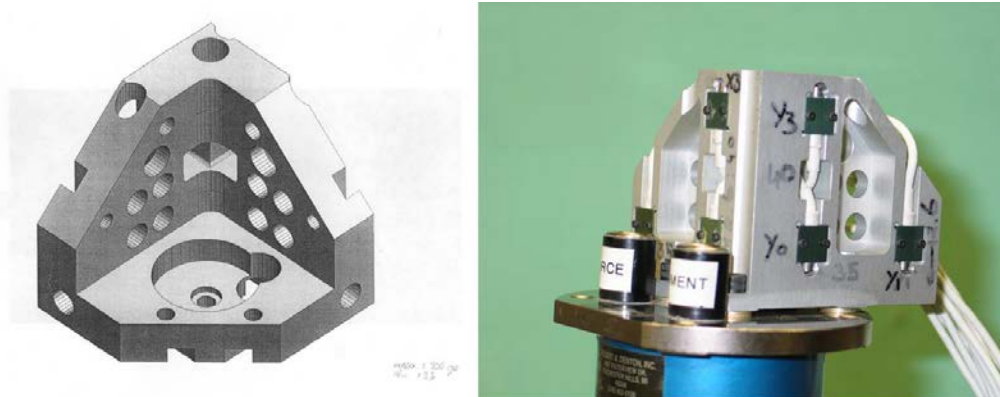


Figure 10: NAP - Left: Isometric View, Right: Embedded Accelerometers

Several additional channels were recorded but are not all reported in this paper due to its focus on head and neck injury. For the forward-facing seat, the FAA Hybrid III was instrumented with chest and pelvis X and Z accelerometers, and a lumbar load cell measuring Fx, Fz, and My. The rigid seat incorporated a load cell under the seat pan that measured the forces and moments exerted on the pan by the ATD (Fx, Fz, and My). These forces were tare compensated using data gathered from a test with no ATD. The tensions on both sides of the lap belt were measured between the pelvis of the ATD and the belt anchor with webbing transducers. For the side facing seat, the additional instrumentation and measurements are documented in the test report [7]. All test data were gathered and filtered per the requirements of SAE J211/1 [14]. The sign convention of the recorded signals conformed to SAE J1733 [15]. The electronic data were recorded for 400 ms.

Video Coverage

High-speed (1000 frames per second), high resolution (1024 x 512 pixels) color video was captured from the side and overhead by Phantom cameras (Vision Research, Stuart, FL), aimed perpendicular to the sled travel. Targets were placed at key points on the ATD and seat to facilitate motion analysis. The position and velocity of selected targeted points were derived from the videos using procedures complying with the requirements of SAE J211/2 [16]. For forward-facing seat tests, 250 ms of video was recorded, while 400 ms was retained for the side-facing seat tests.

Injury Evaluations

For each test, a variety of head and neck injury metrics were evaluated. These metrics include aviation regulatory (HIC), automotive regulatory (such as HIC15 and N_{ij}), and research injury criteria (such as BrIC). These injury metrics have an associated risk of a specific level of injury, typically based on the Abbreviated Injury Scale (AIS). The AIS is an anatomical-based coding system developed by the Association for the Advancement of Automotive Medicine that classifies and ranks the severity of specific injuries [17]. It represents the threat to life associated with the injury rather than the comprehensive assessment of the severity of the injury. An AIS value of two is denoted as moderate, a value of three is denoted as serious, and a value of four is denoted as severe.

Head Injury Criteria (HIC)

HIC is used to evaluate head injury risk and has an FAA regulatory limit of 1000. For HIC36, a value of 1000 corresponds to a 23% risk of an AIS-3 or greater head injury or a 47% risk of an AIS-2 or greater head injury [5]. HIC evolved from the clinically observed prevalence of concomitant concussions in skull fracture cases to relate cadaver impacts to brain injury [18]. It was observed that 80% of all concussion cases also had linear skull fractures and therefore, by limiting the risk of skull fracture, the risk of brain injury is also limited [19]. Prasad and Mertz analyzed the available data and determined the relationship between HIC and injuries to the skull and brain. Based on their methodology, the brain injury relationship resulted in a risk curve nearly identical to the skull fracture injury risk [20].

The original biomechanical skull fracture data was based on short duration impacts where no specimen experienced a HIC duration greater than 13 ms [3]. Additionally, human volunteer tests demonstrated that the probability of injury in long duration events was low [3]. Despite this evidence, the original implementation of HIC did not limit the duration and NHTSA was cautious in subsequently limiting the duration to 36 ms. With the proliferation of airbags, the duration was later limited to 15 ms to compensate for the tendency for HIC to overestimate the injury risk for the long periods of relatively low acceleration produced by airbag contacts.

Four versions of the HIC calculation are included in this report: aviation HIC, HIC15, HIC36, and HIC Unlimited. All four use the same equation (below). The aviation HIC calculation and the HIC Unlimited both have an unlimited duration, but the aviation calculation cited in 14 CFR 25.562 differs from the automotive version in that the resultant head acceleration includes only the data after head contact. Body-to-body contact is excluded from the aviation calculation due to the undamped resonant response that can occur when relatively rigid parts of the ATD strike each other, which may give an artificially high HIC value. HIC15 uses all the data, but the time duration is limited to 15 ms, while HIC36 limits the time duration to 36 ms.

$$HIC = \left\{ (t_2 - t_1) \left[\frac{1}{(t_2 - t_1)} \int_{t_1}^{t_2} a(t) dt \right]^{2.5} \right\}_{max}$$

where t_1 is the initial integration time in seconds, t_2 is the final integration time in seconds, and $a(t)$ is the total acceleration for the head in units of gravity. The values of t_1 and t_2 are selected such that the HIC value is the maximum possible for the time period being evaluated.

Skull Fracture Correlate (SFC)

The Skull Fracture Correlate was developed by NHTSA and the Medical College of Wisconsin solely to evaluate skull fracture [21]. It was found to correlate better to fracture than any of the standard HIC formulations. The SFC is defined as the average acceleration during the HIC 15 interval, with an SFC value of 120 g corresponding to a 15% probability of skull fracture.

Brain Injury Criteria (BrIC)

The Brain Injury Criteria is a kinematic injury criterion developed by NHTSA as a correlate to a subset of traumatic brain injuries (TBI) in which head rotational velocity is believed to be a

primary injury mechanism [22]. During its development, BrIC was correlated to two physical parameters, Cumulative Strain Damage Measure (CSDM) and max principle strain (MPS). These parameters are indicators of injury calculated by finite element models of the skull and brain. Two independent models, the Simulated Injury Monitor (SIMon) and the Global Human Body Modeling Consortium (GHBMC) head model, were used in the criteria's development.

BrIC is calculated using only the measured angular velocity in each orthogonal axis. The critical values for angular velocity are directionally dependent and are independent of the ATD used for measuring them.

$$\text{BrIC} = \sqrt{\left(\frac{\omega_x}{\omega_{xC}}\right)^2 + \left(\frac{\omega_y}{\omega_{yC}}\right)^2 + \left(\frac{\omega_z}{\omega_{zC}}\right)^2}$$

where ω_x , ω_y , and ω_z are maximum angular velocities (calculated irrespective of the time it has occurred) about the X-, Y-, and Z-axes respectively, and ω_{xC} , ω_{yC} , and ω_{zC} are the critical angular velocities in their respective directions. The critical values based on CSDM and MPS are 66.25 rad/s, 56.45 rad/s, and 42.87 rad/s for the X-, Y-, and Z-axes, respectively. A BrIC value of 1.0 corresponds to a 50% probability of AIS 4 or greater anatomic brain injuries.

Neck Injury

Forward-Facing Seat Configuration

To limit the potential for neck injury in forward automotive crashes, 49 CFR 571.208 defines the criteria for neck tension and compression, as well as a criteria that combines the effect of the neck bending moment and axial force, called N_{ij} . This is not currently a pass/fail criterion in aviation but a limit of 1.0 is called out for automotive testing [4]. An N_{ij} value of 1.0 represents a 22% risk of AIS-3 or greater injury for all occupant sizes [3]. The N_{ij} calculation uses force and moment data measured with an upper neck load cell (projected to the occipital condyle location). The automotive regulation also limits compression to 899 pounds and the tension limit is 937 pounds [4].

$$N_{ij} = \frac{F_z}{F_{zC}} + \frac{M_{OCy}}{M_{yC}}$$

F_z is the force at the transition from the head to neck, F_{zC} is the critical force (1530 pounds), M_{OCy} is the total moment, M_{yC} is the critical moment (1200 in-lb).

Side-Facing Seat Configuration

Neck injury criteria for side-facing seats are defined in FAA policy PS-ANM-25-03-R1 [10]. The axial neck tension limit is 405 pound, which represents a 25% risk of an AIS-3 or greater neck injury. The axial compression limit is also 405 pound, which should provide a similar level of safety as the tension limit for this loading condition [23]. Lateral bending moment (M_x) is limited to 1018 in-lb (measured at the occipital condyle location of the ES-2re), which can be considered a threshold below which neck injury is not expected. A limit on the neck shear load of 185 pound represents a 25% risk of an AIS-3 or greater neck injury.

RESULTS

The injury metrics discussed above were calculated using 400 ms of electronic data, except for the angular velocities, and corresponding BrIC, which were calculated based on the first 250 ms. The time period was limited due to some drift issues, which are discussed in the limitations section and the appendix. In the tables, values in italicized red text denote a parameter that exceeds the injury criteria limit.

Forward-Facing Seat Configuration

Inertial Loading Test Configuration

The 4-point belt configuration was run three times (A05044 – A05046), showing consistent results for most of the reported values (Table 2). During loading, the ATD neck bent forward until the chin struck the sternum, then the head rebounded against the headrest. With the exception of BrIC, the head and neck injury parameters produced were about half the limits, with BrIC being close to the limit. The combined shoulder strap tension loads exceeded the 2000 pound criteria limit in all tests. Since high shoulder strap loads correspond to higher torso acceleration, it is likely that these tests produced more head-neck loading than would be found in a certified seat having belt loads within limits. The results for this test configuration suggest that even at the high G impact condition of a Part 23 pilot seat test, the risk of head-neck injury resulting from only inertial loading is not excessive for a well-restrained occupant.

The lap belt only, inertial loading configuration was run twice, once with the legs blocked (A05047) and once with the legs free to flail (A05048). In this configuration, the ATD flailed forward until the torso of the ATD impacted the thighs. After the motion of the torso was arrested, the head continued to travel between the legs in an arc downward, and eventually rearward. In test A05047, the flail restriction of the lower legs kept the upper legs in their nominal position, which resulted in significant contact between them and the upper torso. This contact caused the head to whip between the legs without striking anything. In test A05048, the torso also contacted the upper thighs, but later than in the previous test. As the head was passing between the legs, which had flailed to nearly horizontal, it contacted the left shin, causing high head acceleration spikes in the X and Y directions and significant angular velocity about all three axes (Table 2). The aviation HIC was not calculated since the ATD did not strike a surface other than itself. The limits for HIC15, HIC Unlimited, and BrIC were exceeded in both tests, while HIC36 was exceeded in one of the two tests. The neck injury criteria and the Skull Fracture Correlate (SFC) were below limits for both tests.

Table 2: Inertial Loading Test Configuration

Test Parameter	Criteria Limit	Test Number				
		A05044	A05045	A05046	A05047	A05048
Test Configuration		No Contact	No Contact	No Contact	Torso Contact	Torso Contact
Restraint		4-pt	4-pt	4-pt	Lap	Lap
Impact Vel (ft/s)		42.2	42.1	42.1	44.5	43.8
Sled Acc (g)		26.0	25.4	25.2	16.6	16.2
Aviation HIC	1000	None	None	None	None	None
Duration (ms)		N\A	N\A	N\A	N\A	N\A
HIC15	700	206	197	179	<i>1142</i>	<i>741</i>
HIC15 Duration (ms)		15.0	15.0	15.0	15.0	15.0
HIC36	1000	280	247	208	<i>1768</i>	973
HIC36 Duration (ms)		29.6	36.0	30.7	36.0	36.0
HIC Unlimited	1000	467	440	369	<i>2437</i>	<i>1649</i>
HIC Unl. Duration (ms)		64.0	166.7	65.6	73.4	90.6
SFC	120	45.2	44.3	42.7	89.6	75.2
Angular Vel X (rad/s)		7.4	14.0	7.1	21.9	33.2
Angular Vel Y (rad/s)		-48.5	-45.5	-48.8	-56.8	-53.6
Angular Vel Z (rad/s)		5.0	8.1	16.9	9.8	-31.4
BrIC	1.0	0.87	0.85	0.96	<i>1.08</i>	<i>1.30</i>
Nij	1.0	0.53	0.52	0.56	0.88	0.77
Neck Tension (lb)	937	456	402	447	901	781
Neck Compression (lb)	899	61	69	59	22	13
Combined Shoulder Strap Load (lb)	2000	<i>1202 (R)</i> <i>1187 (L)</i>	<i>1055 (R)</i> <i>1349 (L)</i>	<i>1039 (R)</i> <i>1283 (L)</i>	N\A	N\A

Row-to-Row Test Configuration

The row-to-row configuration using the rigid seat was run three times to evaluate injury risk and repeatability. Up to the point of head contact with the seat back, the ATD overall kinematics and excursion were very similar. The seat back flexion was also similar until the ATD’s hands contacted the seat back. In each case, the seat back flexion prior to head impact differed somewhat, likely due to differences in how much the hands pushed on the seat back. This phenomenon has been documented in similar loading scenarios [24]. The variable seat back flexion affected when and where the head struck the seat back in each test. For test A05049, the forehead contacted the surrogate screen 3 inches above the tray table. For test A05050, the forehead contacted the tray table just below the top edge of the table. For test A05051, the forehead contacted the screen 6 inches above the top of the tray table.

The differences in head strike location resulted in a fair amount of scatter in the results (Table 3). Aviation HIC varied from 774 to 1350, a range that spans low risk to high risk of a severe head injury. HIC15 also spans a wide range, but all three tests exceeded that injury criteria limit. The HIC36 and HIC Unlimited values were generally equal to the aviation HIC values. In test A05049, head contact with the rigid surrogate screen produced a high acceleration spike in all

three of the X-axis accelerometers. It also produced a high spike in one of the three Y-axis accelerometers, which are oriented perpendicular to the direction of impact. In test A05051, the head contact with the screen also produced a high acceleration spike in all three of the X-axis accelerometers but did not produce a similar Y-axis response. The HIC interval for this impact was only 1 ms with an average acceleration of 238 g (Figure 11). Although the HIC for this impact was less than 1000, the SFC was nearly double the limit, suggesting that skull fracture is likely. In all three cases, after the initial contact, the head slid down the seat back as it folded forward. In test A05050, the interaction with the seatback interrupted the downward sliding of the head sufficiently to produce tension and extension moments high enough to result in an N_{ij} just over the limit (Figure 12). As seen in the frame grab, minimal neck extension is evident. BrIC was also high in all three tests but did not exceed the limit.

Table 3: Row-to-Row Test Configuration

Test Parameter	Criteria Limit	Test Number			
		A05049	A05050	A05051	A05052
Test Configuration		Seat Back	Seat Back	Seat Back	Seat Back
Restraint		Lap	Lap	Lap	Lap
Impact Vel (ft/s)		44.4	44.4	44.4	44.5
Sled Acc (g)		16.6	16.6	16.8	17.1
Aviation HIC	1000	774	<i>1350</i>	948	<i>1439</i>
Duration (ms)		15.3	23.6	1.0	10.2
HIC15	700	<i>773</i>	<i>1114</i>	<i>948</i>	<i>1439</i>
HIC15 Duration (ms)		15.0	15.0	1.0	10.2
HIC36	1000	774	<i>1432</i>	948	<i>1439</i>
HIC36 Duration (ms)		15.3	33.7	1.0	10.2
HIC Unlimited	1000	774	<i>1432</i>	948	<i>1439</i>
HIC Unl. Duration (ms)		15.3	33.7	1.0	10.2
SFC	120	85.5	88.6	<i>237.4</i>	118.7
Angular Vel X (rad/s)		8.7	7.0	11.5	20.3
Angular Vel Y (rad/s)		-46.5	-51.4	-39.6	-50.9
Angular Vel Z (rad/s)		5.2	15.1	11.8	17.1
BrIC	1.0	0.84	0.98	0.77	<i>1.03</i>
N_{ij}	1.0	0.80	<i>1.06</i>	0.67	0.76
Neck Tension (lb)	937	636	690	558	772
Neck Compression (lb)	899	90	121	43	179

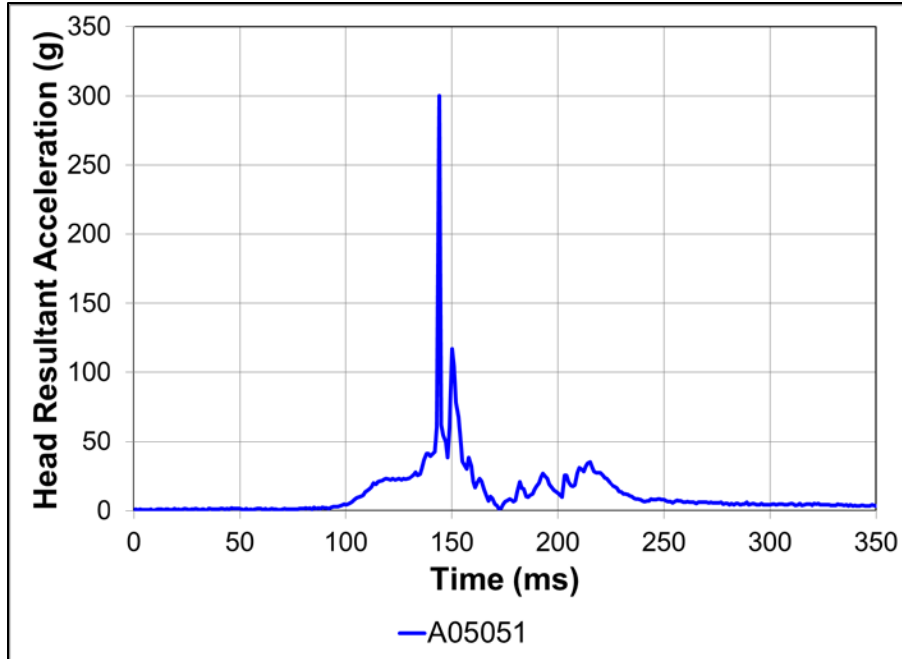


Figure 11: Head Resultant (HIC duration 1 ms)

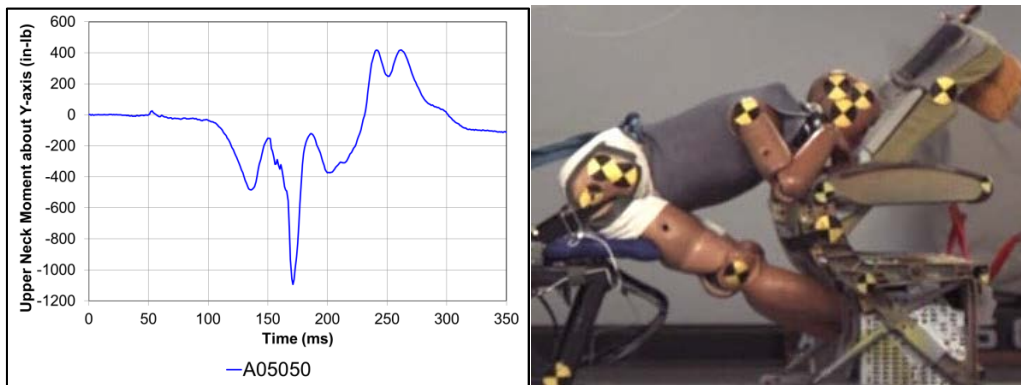


Figure 12: A05050 Upper Neck Moment about Y-axis and Neck Extension at Peak My (171 ms)

The row-to-row configuration using the real seats, test A05052, resulted in a very different interaction between the ATD and the seat back. The inertia force generated by the three ATDs of the forward seat caused the seat rear legs to stroke (as designed), which moved the entire seat frame forward. This moved the seat back hinge point forward, resulting in the head impacting at a much lower point (at the bottom of the tray table) than would have occurred with a seat that was not occupied, or with one having a nearly rigid frame. Conversely, if both seats were fully loaded and stroked the same distance, then the head impact point may be closer to what is produced by rigid frame seats. Contacting at a lower point provides less leverage to actuate the energy absorbing hinge mechanism, which increases the contact force and, therefore, the head acceleration. After contact, the head slid down onto the literature pocket and exhibited significant rotation and neck flexion. This interaction is reflected in the measured HIC of 1439 and BrIC of 1.03. The neck injury criteria, however, were not exceeded which is somewhat surprising given the amount of neck extension observed (Figure 13). This extension was observed over an extended duration (195 ms - 210 ms).

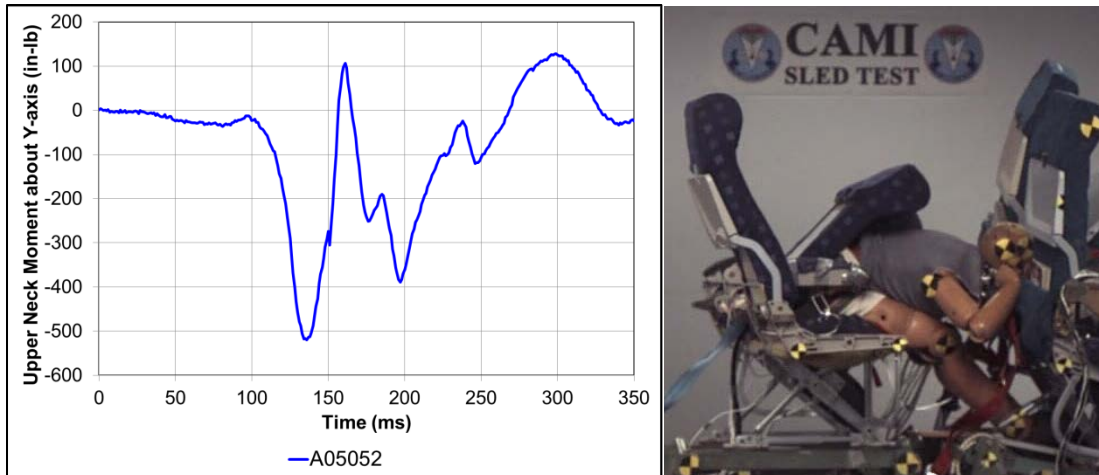


Figure 13: A05052 Upper Neck Moment about Y-axis and Visual Peak of Extension (195-210 ms)

Wall Test Configuration

The wall impact configuration using the rigid seat was run three times to assess injury risk and evaluate repeatability (A05044 – A05046). Up to the point of head contact with the wall, the ATD overall kinematics and excursion were very similar. As in the row-to-row tests, the force of the hands on the wall caused it to deflect forward to varying degrees, affecting the test results. These tests resulted in high values of HIC and BrIC, which generally exceed the defined limits (Table 4). This loading also resulted in high X-axis head acceleration response and high Y-axis response. The validity of that high Y-axis acceleration is suspect because there is nothing in the video to corroborate the high Y accelerations recorded, unlike test A05048 where high Y-axis acceleration coincided with lateral movement of the head due to contact with the leg. The mostly sliding contact with the wall in each case resulted in neck injury parameters below the limits.

Two secondary strike configurations were run (A05057 and A05058). During test A05057, the support angles for the secondary strike surface interfered with the normal arm kinematics of the ATD causing the head to miss the secondary strike target. This resulted in similar kinematics to the three previous wall impact tests; however, the recorded X and Z-axis acceleration coinciding with wall contact was much higher than the previous tests. For test A05058, the strike surface was modified to prevent this interference. During all of the wall impact tests, the head retained significant velocity after interaction with the wall. In test A05058, this caused a very high head acceleration spike of significant duration when the head struck the stiff secondary surface. This test resulted in extreme values for HIC due to the solid head strike on the ledge. Due to very high (likely resonant) response caused by the wall contact and the secondary impact, the head acceleration data was of such poor quality that no angular velocity values were calculated for either of the secondary strike tests.

Table 4: Wall Test Configuration (Forward-Facing)

Test Parameter	Criteria Limit	Test Number				
		A05054	A05055	A05056	A05057	A05058
Test Configuration		Wall	Wall	Wall	Wall + Ledge	Wall + Ledge
Restraint		Lap	Lap	Lap	Lap	Lap
Impact Vel (ft/s)		44.3	44.3	44.3	43.9	44.1
Sled Acc (g)		17.1	16.3	16.3	16.3	16.3
Aviation HIC	1000	974	1560	1202	3581	9659
Duration (ms)		69.2	62.4	65.0	1.2	2.3
HIC15	700	799	632	666	3581	9659
HIC15 Duration (ms)		15	15	15	1.2	2.3
HIC36	1000	923	976	972	3581	9659
HIC36 Duration (ms)		36.0	36.0	36.0	1.2	2.3
HIC Unlimited	1000	1372	1954	1623	3581	9659
HIC Unl. Duration (ms)		105.4	81.7	97.3	1.2	2.3
SFC	120	171.1	77.3	71.8	376.6	437.6
Angular Vel X (rad/s)		-13.3	17.2	17.3	N\A	N\A
Angular Vel Y (rad/s)		-78.9	-66.3	76.7	N\A	N\A
Angular Vel Z (rad/s)		-13.1	-15.5	32.2	N\A	N\A
BrIC	1.0	1.44	1.26	1.57	N\A	N\A
Nij	1.0	0.83	0.74	0.76	0.73	0.92
Neck Tension (lb)	937	691	801	780	726	791
Neck Compression (lb)	899	404	35	251	365	1232

Side-Facing Seat Configuration

Center Test Configuration

For the center seat configuration, the ES-2 is in the middle seat of a triple place couch/sofa (A05066 – A05068 and A05070). With the conventional torso restraint, the ATD rotates sufficiently for the head to contact the seatback through a 4-inch cushion. This resulted in values of HIC, BrIC, neck tension, and neck shear above the respective limits (Table 5). The data from these two tests (A05066 and A05068) show consistent results. The inclusion of an inflatable torso restraint prevents the ATD from impacting the seat, and therefore reduced all the measured injury parameters, although BrIC is close to the limit (0.90 and 0.88).

Table 5: Center Test Configuration

Test Parameter	Criteria Limit	Test Number			
		A05066	A05068	A05067	A05070
Test Configuration		Center	Center	Center	Center
Restraint		Conventional	Conventional	Inflatable	Inflatable
ATD		ES-2	ES-2	ES-2	ES-2
Impact Vel (ft/s)		44.6	44.6	44.5	44.6
Sled Acc (g)		17.4	17.7	17.1	17.4
Aviation HIC	1000	<i>1259</i>	<i>1391</i>	None	None
Aviation HIC Duration (ms)		21.8	24.3	N\A	N\A
HIC15	700	<i>1093</i>	<i>1115</i>	103	96
HIC15 Duration (ms)		15.0	15.0	15.0	15.0
HIC36	1000	<i>1793</i>	<i>1875</i>	200	180
HIC36 Duration (ms)		36.0	36.0	36.0	36.0
HIC Unlimited	1000	<i>1865</i>	<i>1945</i>	241	220
HIC Unl. Duration (ms)		42.9	42.3	69.2	73.7
SFC	120	87.5	88.2	34.2	33.3
Angular Vel X (rad/s)		-74.5	-78.1	-27.6	-32.3
Angular Vel Y (rad/s)		14.6	16.2	25.9	17.8
Angular Vel Z (rad/s)		-13.9	-22.6	-27.9	-28.2
BrIC	1.0	<i>1.20</i>	<i>1.32</i>	0.90	0.88
Neck Tension (lb)	405	<i>752</i>	<i>729</i>	297	319
Neck Compression (lb)	405	6	7	12	321
Neck Bending Mx (in-lb)	1018	382	381	402	347
Neck Shear Fxy (lb)	186	<i>252</i>	<i>276</i>	111	127

Wall Test Configuration

In the close wall configuration, A05056, the ES-2 ATD is seated 3 inches from a rigid, padded wall while wearing a conventional 3-pt restraint. During the test, the ATD remained completely upright and all the injury parameters are fairly low (Table 6). The far wall configuration was identical, except the ATD is 6 inches from the wall (A05071 and A05072). This allowed for the head to accelerate prior to contacting the wall, resulting in high HIC and SFC values, although BrIC was low. The ATD did stay upright, which kept the other injury parameters low. The inclusion of an inflatable restraint, A05072, did not prevent head contact with the wall, but did slow the ATD down enough to greatly reduce the HIC scores (145 vs. 2014).

Table 6: Wall Test Configuration (Side-Facing)

Test Parameter	Criteria Limit	Test Number		
		A05065	A05071	A05072
Test Configuration		Close Wall	Far Wall	Far Wall
Restraint		Conventional	Conventional	Inflatable
ATD		ES-2	ES-2	ES-2
Impact Vel (ft/s)		44.0	44.6	44.6
Sled Acc (g)		16.4	16.8	17.0
Aviation HIC	1000	537	2014	145
Aviation HIC Duration (ms)		6.4	4.6	14.7
HIC15	700	537	2014	151
HIC15 Duration (ms)		6.4	4.6	15.0
HIC36	1000	537	2014	205
HIC36 Duration (ms)		6.4	4.6	36.0
HIC Unlimited	1000	537	2014	206
HIC Unl. Duration (ms)		6.4	4.6	39.8
SFC	120	92.6	178.9	39.9
Angular Vel X (rad/s)		-30.1	-42.0	-44.5
Angular Vel Y (rad/s)		18.7	14.4	15.5
Angular Vel Z (rad/s)		10.2	12.4	8.4
BrIC	1.0	0.61	0.74	0.75
Neck Tension (lb)	405	140	282	290
Neck Compression (lb)	405	162	64	6
Neck Bending Mx (in-lb)	1018	141	510	625
Neck Shear Fxy (lb)	186	124	152	68

Armrest Test Configuration

The armrest condition resulted in extreme flail, but essentially no head contact (only contact was with shoulder). This is a function of a lack of surrounding structure more than any other circumstance. In the two tests with a conventional restraint system, A05075 and A05076, the automotive HIC values suggest that injury could occur (Table 7). Likewise, BrIC and the neck parameters suggest severe injury. The FAA Hybrid III was also tested in this configuration (A06004). While the ATD torso had similar kinematics to the ES-2, the Hybrid-III's neck is much stiffer and less biofidelic in lateral bending, which resulted in reduced head kinetics. Therefore, the FAA Hybrid III HIC, BrIC, and neck loads are provided for reference only. The defined neck criteria limits are not applicable to that ATD, and the lack of lateral bending biofidelity reduces the confidence that the HIC and BrIC results measured using this ATD reflect the actual injury risk for this occupant loading condition.

Table 7: Armrest Test Configuration

Test Parameter	Criteria Limit	Test Number				
		A05075	A05076	A05073	A05074	A06004**
Test Configuration		Armrest	Armrest	Armrest	Armrest	Armrest
Restraint		Cnv*	Cnv*	Inflatable	Inflatable	Cnv*
ATD		ES-2	ES-2	ES-2	ES-2	FAA HIII
Impact Vel (ft/s)		45.1	45.1	45.1	45	45.2
Sled Acc (g)		17.1	16.5	17.4	17.4	17.3
Aviation HIC	1000	None	None	None	None	None
Aviation HIC Duration		N\A	N\A	N\A	N\A	N\A
HIC15	700	<i>735</i>	614	84	79	157
HIC15 Duration (ms)		15.0	15.0	15.0	15.0	15.0
HIC36	1000	<i>1198</i>	<i>1104</i>	153	147	307
HIC36 Duration (ms)		36.0	36.0	36.0	36.0	36.0
HIC Unlimited	1000	<i>1214</i>	<i>1161</i>	177	174	423
HIC Unl. Duration (ms)		48.1	52.7	63.4	69.0	70.7
SFC	120	75.1	70.0	31.5	30.7	40.5
Angular Vel X (rad/s)		-82.	-83.5	-24.8	-20.3	-36.8
Angular Vel Y (rad/s)		-20.3	-29.3	16.0	17.5	-14.3
Angular Vel Z (rad/s)		-20.3	29.3	-12.1	-13.3	14.4
BrIC	1.0	<i>1.38</i>	<i>1.52</i>	0.55	0.53	0.70
Neck Tension (lb)	405	<i>789</i>	<i>735</i>	289	271	430
Neck Compression (lb)	405	4	6	7	5	11
Neck Bending Mx (in-lb)	1018	668	681	414	394	595
Neck Shear Fxy (lb)	186	<i>231</i>	<i>216</i>	87	75	220

* Conventional restraint system

** HIII response provided for reference only

The inflatable restraint tests, A05073 and A05074, did not result in head contact. The various head and neck injury parameters are all well below the criteria limits. Similar to the row-to-row example (A05052), neck bending that may appear injurious does not always result in high loads (Figure 14).

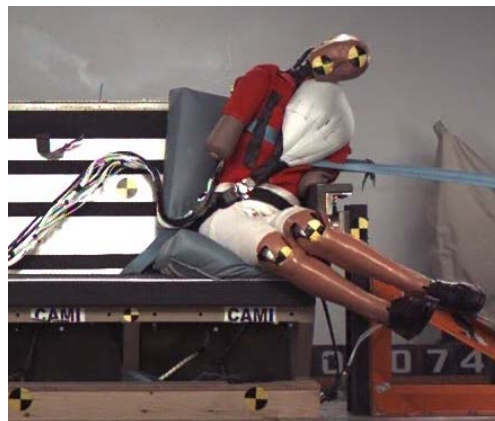


Figure 14: A05074 Max Head Excursion (t=158 ms)

DISCUSSION

Neck Injury

Neck injury was not a significant risk in most of the forward facing seat configurations tested. The N_{ij} exceeded the Federal Motor Vehicle Safety Standards limit in only one case: a row-to-row test where the point of head contact was the tray table (A05050). In this case the interaction was significant enough to exceed all of the HIC limits and nearly exceed the BrIC limit. Peak tension and compression values were not exceeded in any of the typical loading scenarios. The compression limit was only exceeded in the case where the ATD hit a secondary ledge and generated a HIC of 9659. These tests suggest that as long as the head is protected, the neck will be as well. However, subsequent testing has demonstrated that this is not true if the ATD chin catches on a tray table or other seat feature during the occupant's forward flail [24].

Neck injury was a significant risk in some of the side facing configurations tested. The neck and shear force limits defined in FAA policy PS-ANM-25-03-R1 were exceeded in many of the seat configurations. Essentially, any of the configurations that did not provide support to the head and neck by means of a padded wall or inflatable restraint generated excessive neck forces.

Head Injury

Head injury risk was significant in many of the configurations, even though the seats incorporated features to reduce the risk of head injury. Some of the factors contributing to increased head injury risk were:

- Lap belt restrained occupants – inertial loading: Excessive head rotational velocity as the head whips downward after the chest impacts the upper legs. Contact with lower leg as the head travels between the extended legs.
- Row-to-row impacts: Inconsistent performance of energy absorbing seat back due to interaction with the ATD's arms. Varying impact point on seat back due to stroking of the target seat legs.
- Wall impacts: Insufficient energy absorbed by the wall contact permitted similar injury response as in the lap belt restrained inertial loading case. Interaction with the ATD's arms contributed to inconsistent head interaction with the wall.
- Side-facing seats: Lack of upper body support resulted in contact with surrounding surfaces or excessive head rotation.

Brain Injury

In the paper detailing BrIC, the authors observed that “BrIC is a rotational injury criterion, while HIC is a translational injury criterion (calculated using translational accelerations only), and combining the two may better capture head injuries. However, a human head is rarely experiencing just rotational or just translational motion. It usually is experiencing both [22].” Using these criteria to independently assess the two types of injury risk (skull fracture and traumatic brain injury) may be a big step forward in predicting head injury; however, they may not capture all possible injuries, particularly if the injury is a result of a combined loading condition.

To evaluate the utility of the two assessments, a pass or fail was considered for each test based on an aviation HIC limit of 1000 and a BrIC limit of 1.0 (Figure 15). In nine cases, the tests either pass both or fail both. In only one test was the aviation HIC below the limit of 1000 while BrIC was over the 1.0 limit. This was a wall impact (A05054), which had an aviation HIC of 974, a BrIC of 1.44, and values of HIC15, HIC Unlimited, and SFC above the respective limits. This test was run two more times and aviation HIC and BrIC were exceeded in each. Based on this limited sample, BrIC does not appear to capture a risk of injury beyond that of the current regulatory criteria for these configurations.

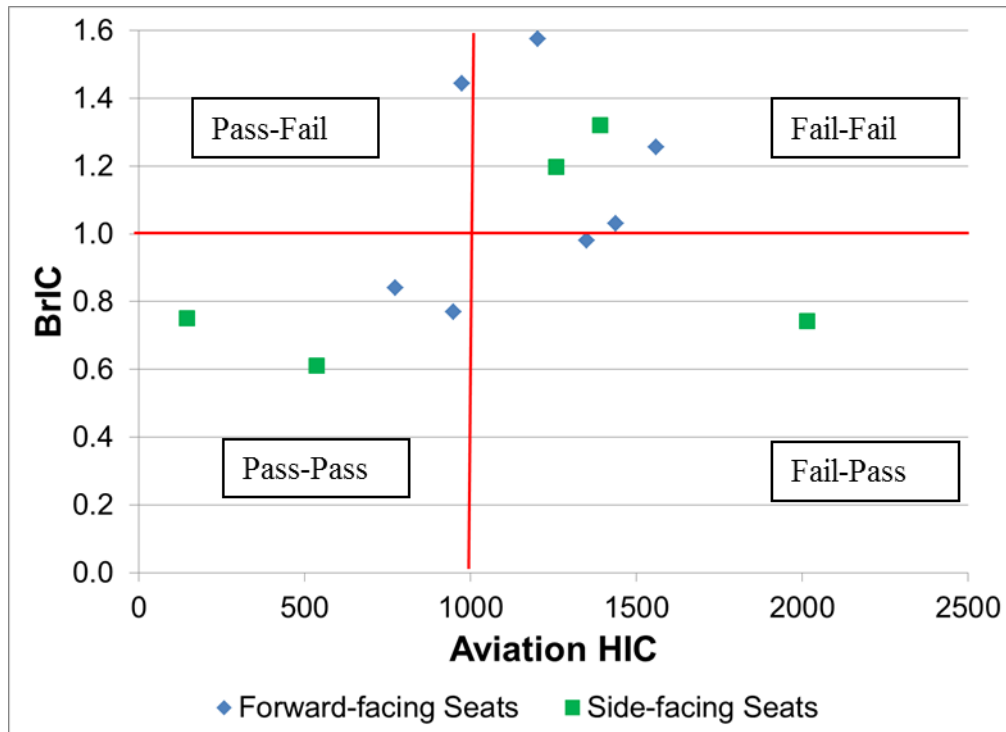


Figure 15: Aviation HIC vs. BrIC

The added safety benefit of the BrIC calculation may lie in the scenarios where aviation HIC is not calculated. In the five forward facing seat tests with no contact besides dummy-to-dummy, BrIC was exceeded in the two lap belt only tests and was 0.85 or greater in the three tests with a 4-pt restraint. For the side-facing seats, the two tests in a center seat place with an inflatable restraint had a BrIC near the limit (0.88 or greater), while all the other injury criteria were low. For the side-facing armrest tests with a conventional belt, BrIC was well above the limit, as were the other versions of HIC and the neck injury criteria. This sample suggests that aviation HIC may miss some potentially injurious configurations, although this can be partially offset by the neck injury criteria for side-facing seats.

Considering that the derivation of HIC was primarily based on short duration impacts (between 3 ms and 12 ms) and that NHTSA has adopted HIC15, aviation HIC was compared to HIC15 to see the impact of using HIC15 to determine whether a test passed or failed (Figure 16). In this evaluation, two tests had an aviation HIC over 1000 while HIC15 was under 700. Both of

these tests were the wall impact configuration. Interestingly, this is the opposite result of the other test in this configuration (A05054) which had aviation HIC below 1000, but HIC15 above 700 (as discussed above). In three tests, HIC15 is above 700 while aviation HIC is below 1000, including two row-to-row seatback tests where all four versions of HIC produced the same result (A05049 and A05051), and one of the wall impact tests (A05054). Not included in this comparison are the twelve tests where aviation HIC is not calculated, of which three fail HIC15. Based on this limited sample, it appears that a switch from aviation HIC to HIC15 would result in a shift in the configurations that meet the rule. Further research is needed to understand the impact of this shift and determine if there is a safety benefit to adopting a different HIC formulation.

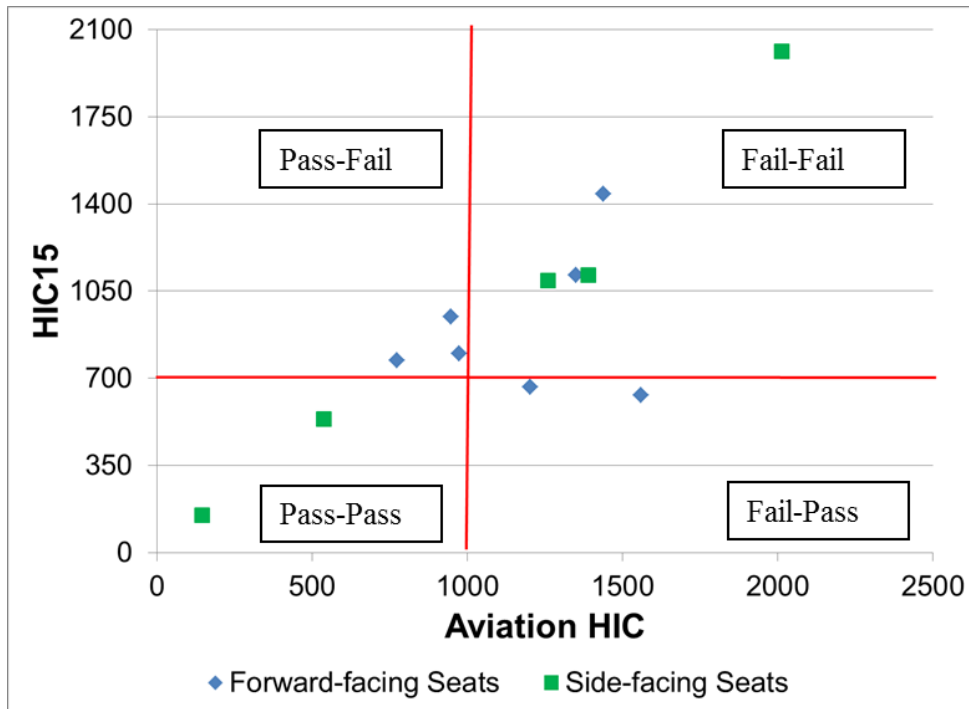


Figure 16: Aviation HIC vs. HIC15

LIMITATIONS

As an exploratory study, the number of impact scenarios investigated was limited. The seat configurations selected were those that were commonly found in general aviation and transport aircraft at the time of the study. However, there may be configurations that can produce impacts with different injury risks. Specifically, varying parameters such as seat back stiffness and row-to-row spacing can affect both the head and neck injuries produced. Interaction with some airbag configurations may also produce injuries and warrant further study. The scope of this report was limited to evaluating only head-neck injuries; other injury criteria may have been exceeded in some tests even if the head and neck injury criteria were within limits.

The nine-accelerometer array package (NAP) uses differences between linear accelerometers as detailed in the Appendix. The raw rotational velocities derived during this project have cumulative error (drift) across their time history. The source of this drift is the 12-bit resolution analog-to-digital conversion (A/D) data acquisition system used in this study. While methods were employed to significantly improve the accuracy by empirically compensating for the drift,

as detailed in the Appendix, the angular velocities reported, and BrIC values based on them, should be considered estimates only. Any further studies evaluating brain injury should be conducted using newer and more accurate technology such as angular rate sensors, or a NAP array connected to a 16-bit or greater A/D data acquisition system.

Some of the head contacts involving impacts onto locally rigid surfaces resulted in very high, short duration acceleration spikes, including ones registered by accelerometers that were oriented 90 degrees to the impact direction. In product development tests, this type of response is often observed during impacts with seat back mounted video monitors. The mechanism producing these data spikes has recently been attributed to the resonant response of undamped accelerometers, which can resonate during impacts onto rigid structures [14]. Even when whole body acceleration is expected to be below 500 g, the resonance can produce amplitudes much greater than 500 g. When the data acquisition system is set to a range of 500 g for a given transducer, resonance can cause severe data distortion. Information on this phenomenon was included in the 2014 version of SAE J211, along with a discussion of damped vs. undamped accelerometers [14]. In this test series, 2000 g accelerometers were used in the head, but they were set to the typical 500 g range, so resonant response could account for the high magnitude, short duration responses measured during rigid impacts. Currently, there is no definitive answer as to whether very short duration impacts have sufficient energy content to produce injury. However, when Prasad and Mertz analyzed available test data to determine the relationship between HIC and injuries to the skull and brain, the HIC durations ranged from 0.9 to 10.1 msec [20]. From their analysis we can infer that HIC durations of at least 1 ms long were considered biomechanically valid. Further research is needed to better understand the accuracy of the measured accelerations and the injury risks posed by these types of contacts.

CONCLUSION

A series of 26 tests across 6 typical aircraft seat and interior configurations during aircraft forward impact conditions were conducted to assess the potential of head and neck injury. These tests used specialized instrumentation to evaluate a range of metrics that include both regulatory and non-regulatory (research) injury criteria.

Neck injury was not a significant risk in most of the forward-facing seat configurations tested. This included cases where the neck bending visually appears injurious, but did not result in high measured loads. For the side-facing seat configurations, neck injury was a significant risk, particularly for seating systems that did not provide effective upper body support. The 2012 FAA policy for side-facing seats was implemented, in part, to address this risk.

For head injury, there was significant overlap between the aviation HIC and BrIC pass/fail determinations, suggesting that BrIC does not capture a risk of injury beyond that of the current regulatory criteria for configurations where the head strikes a seatback or monument. However, BrIC did suggest the potential for injury in several tests where the ATD did not contact anything other than itself. When comparing aviation HIC to HIC15, many tests produced a different pass/fail determination depending on which criteria was used. Prior to considering any comprehensive change in FAA policy, further research is needed to understand the impact of this shift and determine if there is a safety benefit to adopting a different HIC formulation. Overall, these results indicate that combining HIC and BrIC to evaluate seating systems could provide a safety benefit by directly evaluating the risk of skull fracture and traumatic brain injury.

REFERENCES

1. US Code of Federal Regulations, Title 14, Part 25.562. Airworthiness Standards: Transport Category Airplanes, Emergency Landing Conditions. Washington, DC: US Government Printing Office, 1988.
2. US Code of Federal Regulations, Title 14, Part 23.562. Airworthiness Standards: Transport Category Airplanes, Emergency Landing Conditions. Washington, DC: US Government Printing Office, 1988.
3. Eppinger R, Sun E, Bandak F, Haffner M, Khaewpong N, Maltese M, Kuppa S, Nguyen T, Takhounts E, Tannous R, Zhang A, Saul R. Development of Improved Injury Criteria for the Assessment of Advanced Automotive Restraint Systems – II. Washington, DC: US Government Printing Office, 1999.
4. US Code of Federal Regulations, Title 49, Part 571.208. Occupant Crash Protection. Washington, DC: US Government Printing Office, 2011.
5. Kuppa S. Injury Criteria for Side Impact Dummies, Washington, DC: DOT/National Highway Traffic Safety Administration; May 2004. FMVSS-214 NPRM docket: NHTSA-2004-17694.
6. SAE International. Aerospace Standard 8049B. Performance standard for seats in civil rotorcraft, transport aircraft, and general aviation aircraft. Warrendale, PA: SAE International, 2005.
7. DeWeese R, Moorcroft D, Green T, Philippens M.M.G.M. Assessment of Injury Potential in Aircraft Side-Facing Seats Using the ES-2 Anthropomorphic Test Dummy. Washington DC: Federal Aviation Administration May 2007; Report No. DOT/FAA/AM-07/13.
8. Gowdy V, DeWeese R, Beebe M, Wade B, Duncan J, Kelly R, Blaker J. A Lumbar Spine Modification to the Hybrid III ATD for Aircraft Seat Tests. Warrendale, PA: SAE International, 1999.
9. Federal Aviation Administration Policy AIR-100-3-3-2000 - Use of Hybrid III Anthropomorphic Test Dummy in Seat Dynamic Testing. Washington, DC: Federal Aviation Administration, 2000.
10. Federal Aviation Administration Policy ANM-25-03-R1 - Technical Criteria for Approving Side-Facing Seats. Washington, DC: Federal Aviation Administration, 2012.
11. US Code of Federal Regulations, Title 49, Part 571.214. Side Impact Protection. Washington, DC: US Government Printing Office, 2011.
12. U.S. Code of Federal Regulations, Title 49, Part 572. Washington, DC: U.S. GPO, Anthropomorphic Test Devices Dummy 50th Percentile Adult Male and SID–II's Side Impact Crash Test Dummy 5th Percentile Adult Female; Final Rules; Federal Register / Vol 71, No. 240 page 75304, Dec 14, 2006.
13. Kuppa S, Eppinger R, McKoy F, Nguyen T, Pintar F, Yoganandan N. Development of Side Impact Thoracic Injury Criteria and their Application to the Modified ES-2 Dummy with Rib Extensions (ES-2re), Stapp Car Crash Journal, Stapp Association, pp. 189-210, Vol. 47. 2003.

14. SAE International. Instrumentation for Impact Test – Part 1- Electronic Instrumentation. Warrendale, PA: SAE International; 2014; Surface Vehicle Recommended Practice No: J211/1.
15. SAE International. Sign Convention for Vehicle Crash Testing. Warrendale, PA: SAE International; Dec. 1994; SAE Surface Vehicle Information Report No: J1733.
16. SAE International. Instrumentation for Impact Test – Part 2- Photographic Instrumentation. Warrendale, PA: SAE International; 2014; SAE Surface Vehicle Recommended Practice No: J211/2.
17. The Abbreviated Injury Scale 2005 - Update 2008, Barrington, Illinois, Association for the Advancement of Automotive Medicine, 2008.
18. Gurdjian ES, Webster JE, and Lissner HR. Observations on the Mechanism of Brain Concussion, Contusion, and Laceration. *Surg., Gynec., & Obstet.* 101: 680-690, 1955.
19. Melvin JW, Lighthall JW, and Ueno K. Brain Injury Biomechanics, in *Accidental Injury: Biomechanics and Prevention*, Nahum and Melvin, Editors. 1993, Springer-Verlag: New York. p. 268-291, 1993.
20. Prasad P and Mertz H. The Position of the United States Delegation to the ISO Working Group 6 on the Use of HIC in the Automotive Environment. SAE Government/Industry Meeting and Exposition, SAE paper no. 851246, 1985.
21. Vander Vorst M, Stuhmiller J, Ho K, Yoganandan N, and Pintar F. Statistically and Biomechanically Based Criterion for Impact-Induced Skull Fracture. *Annual Proceedings of the Association for the Advancement of Automotive Medicine.* 2003; 47: 363–381.
22. Takhounts E, Craig M, Moorhouse K, McFadden J, and Hasija V. Development of brain injury criteria (BrIC). *Stapp Car Crash Journal.* 57, 243–266. 2013.
23. DeWeese R, Moorcroft D, Abramowitz A, Pelletiere J. Civil Aircraft Side-Facing Seat Research Summary. Washington DC: Federal Aviation Administration Nov. 2012; Report No. DOT/FAA/AM-12/18.
24. Taylor AM, DeWeese RD, Moorcroft DM. Effect of Passenger Position on Crash Injury Risk in Transport-Category Aircraft. Washington DC: Federal Aviation Administration Sept. 2015; Report No. DOT/FAA/AM-15/17.
25. Padgaonkar A, Krieger K, King A. Measurement of angular acceleration of a rigid body using linear accelerometers. *Journal of Applied Mechanics,* pp. 552-556. 1975.

APPENDIX

Angular Velocity Derivation

To evaluate brain injury, angular data from the head CG is needed. Angular velocity data is acquired in one of two methods: direct measurement with angular rate sensors or derived from a set of 9 linear accelerations. At the time of this test series, angular rate sensors were not readily available. To generate the necessary data, a 9-accelerometer array package (NAP) was used. The 9 linear accelerations were then processed to generate angular accelerations and integrated to produce angular velocity (linear velocity was also calculated). A custom Matlab script was written by M. Philippen, TNO, to process the data. Filtered data (CFC 1000) was used for all inputs into the equations.

NAP Calculations

Rigid body dynamics principles are used to convert linear accelerations from nine accelerometers placed in a 3-2-2 configuration to angular motion of a rigid body. For a rigid body, the 3D motion of point B measured by an observer located at point A (Figure A1) is the same as the motion of that body about a fixed point.

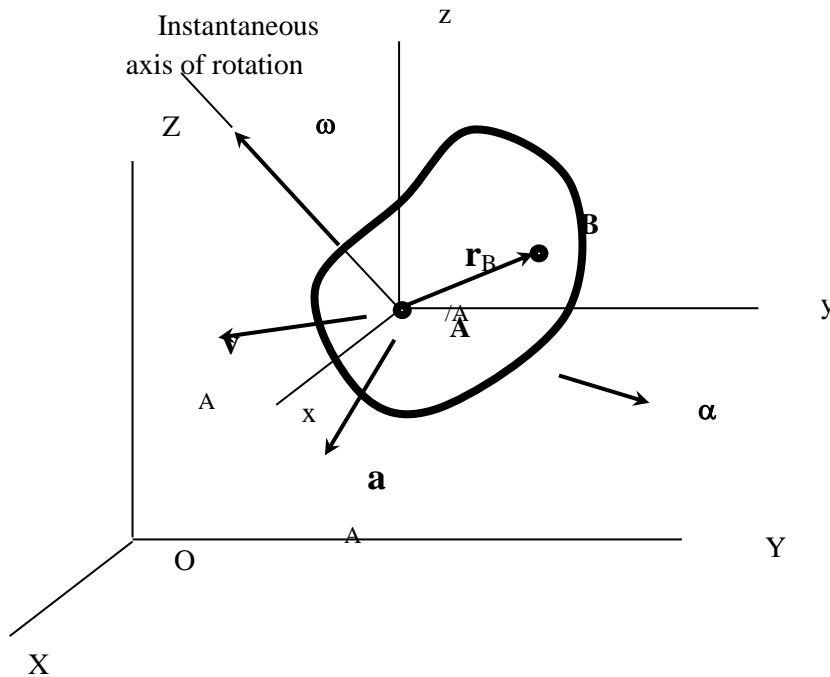


Figure A1: Rigid Body Motion

The absolute acceleration of point B is:

$$\mathbf{a}_B = \mathbf{a}_A + \boldsymbol{\alpha} \times \mathbf{r}_{B/A} + \boldsymbol{\omega} \times (\boldsymbol{\omega} \times \mathbf{r}_{B/A})$$

In component form, this becomes:

$$\begin{bmatrix} a_{Bx} \\ a_{By} \\ a_{Bz} \end{bmatrix} = \begin{bmatrix} a_{Ax} \\ a_{Ay} \\ a_{Az} \end{bmatrix} + \begin{bmatrix} \alpha_y r_z - \alpha_z r_y \\ \alpha_z r_x - \alpha_x r_z \\ \alpha_x r_y - \alpha_y r_x \end{bmatrix} + \begin{bmatrix} \omega_x (\omega_y r_y + \omega_z r_z) - r_x (\omega_y^2 + \omega_z^2) \\ \omega_y (\omega_z r_z + \omega_x r_x) - r_y (\omega_z^2 + \omega_x^2) \\ \omega_z (\omega_x r_x + \omega_y r_y) - r_z (\omega_x^2 + \omega_y^2) \end{bmatrix}$$

The nine accelerometer array package placed in a 3-2-2-2 configuration is shown in Figure A2 where r_x is denoted as r_1 , r_y is denoted as r_2 , and r_z is denoted as r_3 .

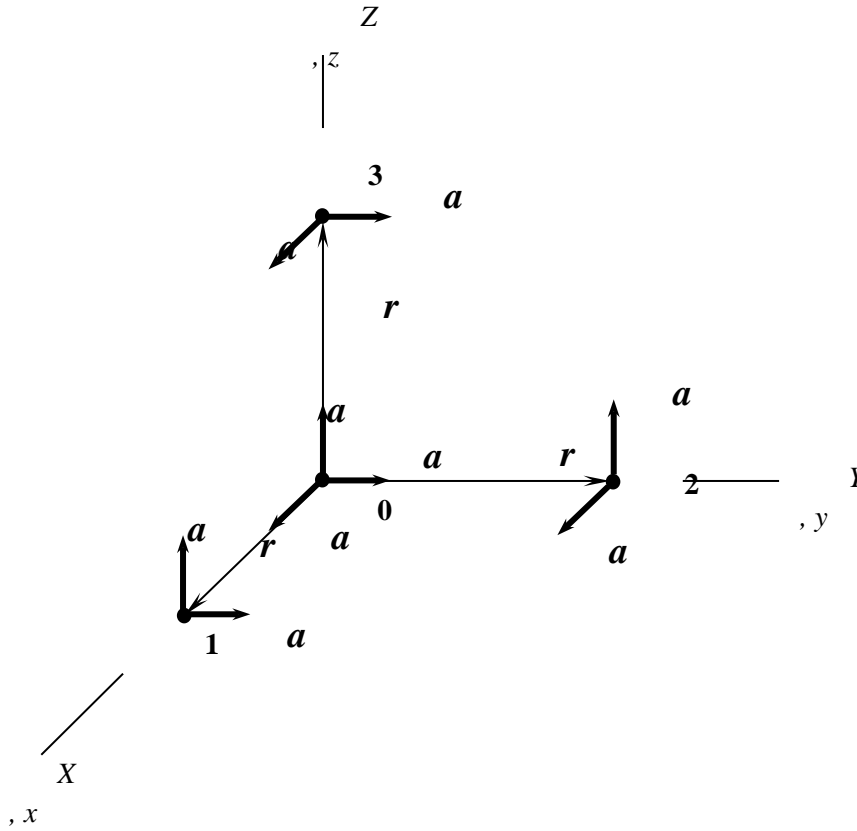


Figure A2: Nine Accelerometer Array Configuration

Knowing the arm lengths and solving for angular acceleration, yields:

$$\begin{cases} \alpha_x = \frac{a_{2z} - a_{0z}}{2r_{y1}} - \frac{a_{3y} - a_{0y}}{2r_z} \\ \alpha_y = \frac{a_{3x} - a_{0x}}{2r_z} - \frac{a_{1z} - a_{0z}}{2r_x} \\ \alpha_z = \frac{a_{1y} - a_{0y}}{2r_x} - \frac{a_{2x} - a_{0x}}{2r_{y2}} \end{cases}$$

Where $r_x = 1.378$ inches, $r_{y1} = 1.524$ inches, $r_{y2} = 1.378$ inches and $r_z = 1.860$ inches. In theory, only a single r_y value is necessary, however in the physical NAP used in this study, the moment arms were different. These equations are given in Padgaonkar et al. and currently serve as the basis for derivation of angular motion of a rigid body from a set of nine linear accelerations [24]. Since these linear accelerations are a function of time, the angular velocities of the rigid body could be obtained by simply integrating with respect to time:

$$\begin{cases} \omega_x(t) = \int_t \alpha_x(t) dt \\ \omega_y(t) = \int_t \alpha_y(t) dt \\ \omega_z(t) = \int_t \alpha_z(t) dt \end{cases}$$

NAP Corrections

Small errors in the difference routines in the NAP algorithm can multiply the errors causing signal drift. At the time of data collection, the DAQ system used by CAMI was an older 12 bit Analog to Digital (A/D) converter (DTS TDAS 2, Seal Beach, CA). A 12 bit system has 4096 steps (2^{12}), which is a much lower resolution than current 16 bit A/D converters, which have 65,536 steps (2^{16}). This results in a relatively high noise floor and a noticeable drift in angular velocity calculations (Figure A4). These errors were compensated by setting boundary conditions and comparing results with photometric analysis results.

Test video was observed to determine a time when the ATD head had zero angular velocity. A routine in Matlab (inte2.m) was used to calculate the integral of the angular acceleration while applying the boundary condition (i.e. angular velocity equal zero at time t). For the tests reported herein, the time selected was either 45 ms for forward-facing tests or 90 ms for side-facing tests. The boundary condition was defined for all three directions. The routine outputs the corrected angular velocity and the offset applied to the angular acceleration. This offset was then added to the original angular acceleration.

Example 1: Test A05044 (forward facing, 4-point belt)

As seen in the video of the test (Figure A3), the ATD head rotates forward starting at about 50 ms. Therefore, 45 ms was selected as an appropriate boundary condition time. At approximately 127 ms the forward rotation of the head stops and reverses as the torso momentum is halted by the shoulder straps. The head rebounds back until approximately 220 ms when the head makes contact with the head rest. The head then rotates forward before coming to a final rest at a time greater than 350 ms (the saved video was limited to 250 ms). Figure A4 shows the calculated angular velocity with no boundary conditions applied. The drift of the signal is clear as the final y-axis angular velocity of the head is reported to be approximately 20 rad/s.

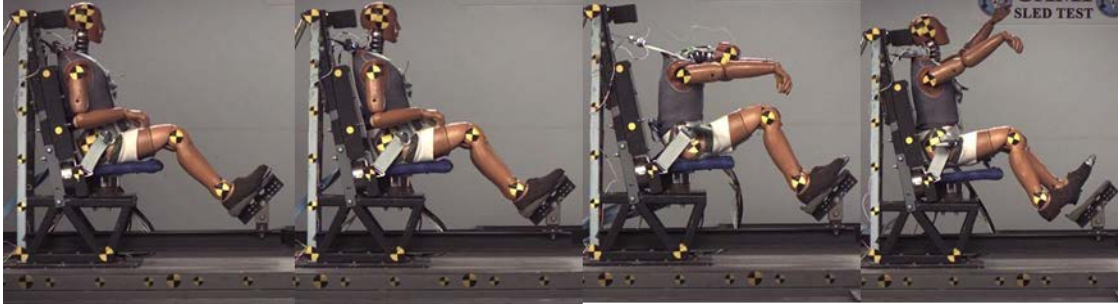


Figure A3: Test A05044 at 0 ms, 45 ms, 127 ms, and 220 ms

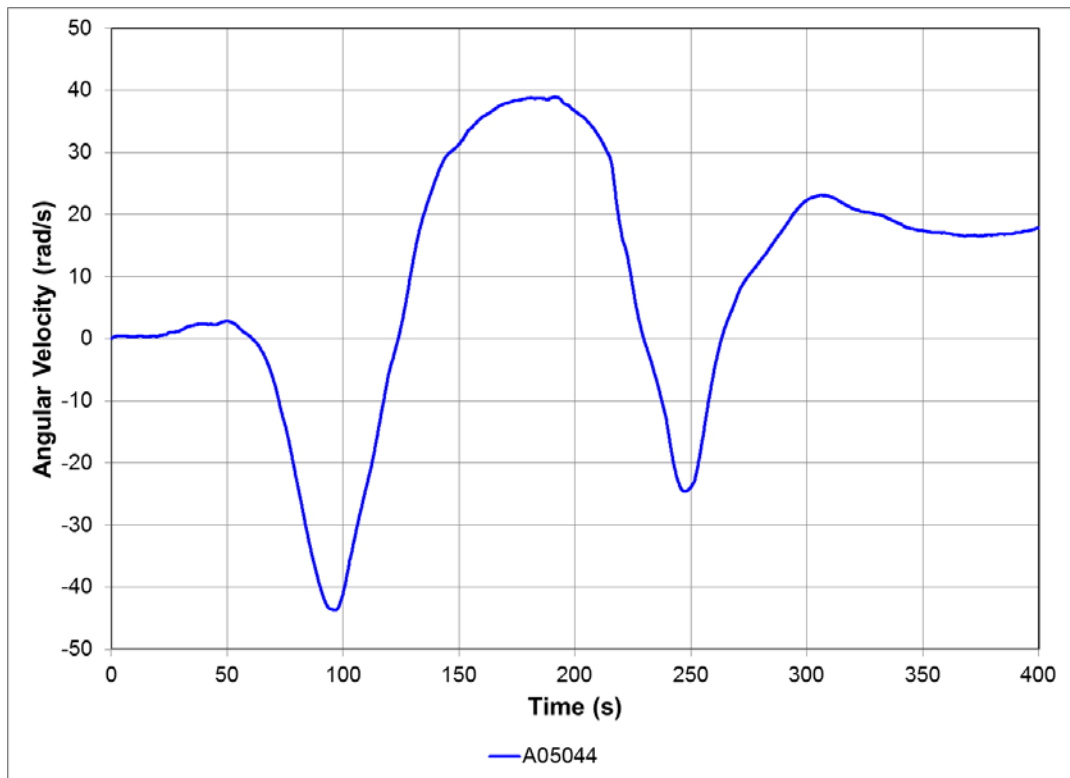


Figure A4: Raw Angular Velocity about Y-axis with Drift

Figure A5 shows the corrected head angular velocity about the y-axis. In agreement with the video, the data crosses zero at approximately 127 ms and 220 ms. The figure also shows the calculated angular velocity from photometrics, which has a calculated accuracy of 0.05 inch per SAE J211-2. There is good agreement (5% error per the Sprague and Geers Comprehensive error) between the two curves suggesting that the velocity correction was accurate.

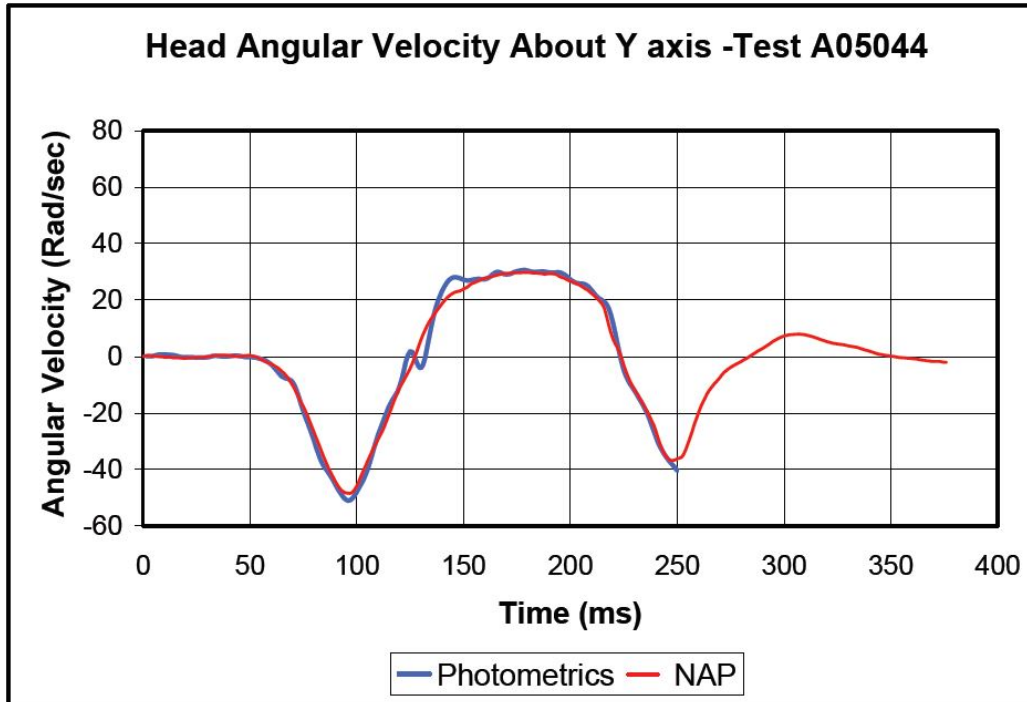


Figure A5: Corrected NAP data vs Photometric

Example 2: Test A05046 (Forward facing, 4-point belt)

After correction, some tests still demonstrated signal drift. Most noticeable is the z-axis angular velocity for test A05046 (Figure A6). All three axes have zero angular velocity through 50 ms and the X and Y axes are close to zero at 400 ms. Conversely, the z-axis has nearly 30 rad/s of final angular velocity. The corresponding video does not show any twist of the head, through 250 ms, to corroborate the data (Figure A7). Considering that the slope of the z-axis angular velocity is essentially constant from 75 ms to 400 ms, this is considered drift. Some other tests demonstrated a similar response, leading the authors to limit the angular velocity calculations to 250 ms, which corresponds to the length of the saved videos.

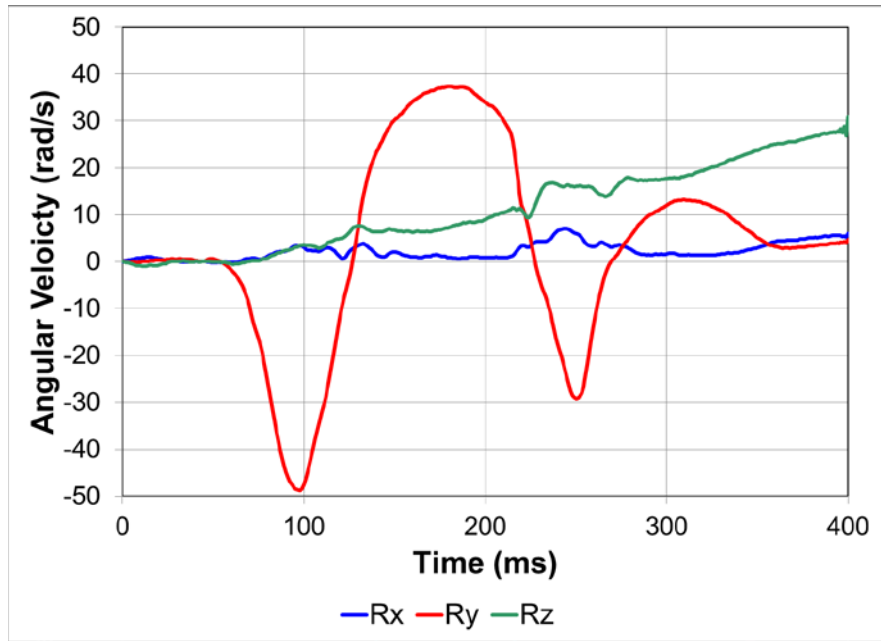


Figure A6: Head Angular Velocity for A05046

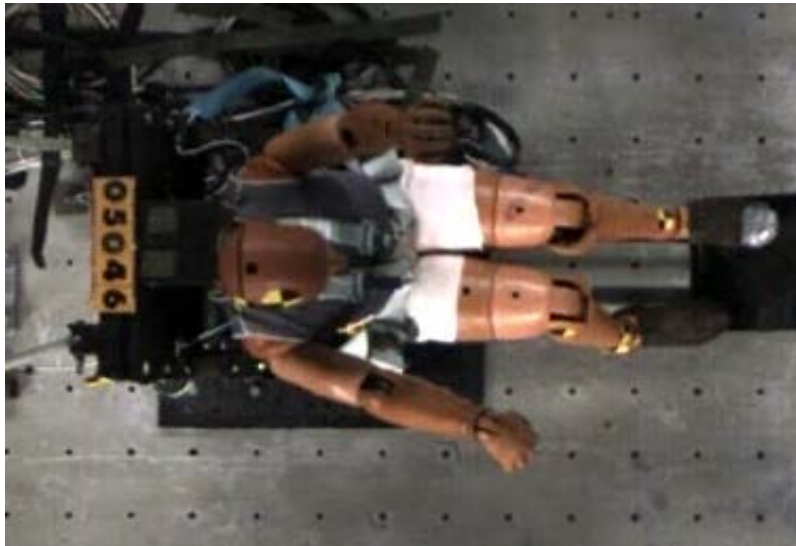


Figure A7: Test A05046 at 250 ms